JOURNAL OF MATERIALS SCIENCE **38** (2003) 3437–3447

Elevated temperature tensile properties and failure of a copper-chromium *in situ* composite

K. L. LEE*, †, A. F. WHITEHOUSE
Department of Engineering, University of Leicester, University Road, Leicester LE1 7RH, UK
E-mail: kokloong1@hotmail.com

A. M. RUSSELL, K. WONGPREEDEE
Materials Science and Engineering Department, Iowa State University, Ames, IA, 50011, USA

S. I. HONG
Department of Metallurgical Engineering, Chungnam National University, Taedok Science Town, Taejon 305-764, Korea

P. J. WITHERS
Manchester Materials Science Centre, Grosvenor St., Manchester M1 7HS, UK

A Cu-10 vol% Cr *in situ* composite was produced by melt processing and deformed by swaging to form rods with a total deformation true strain of 3.15. Scanning electron microscopy showed that the composite microstructure consisted of Cr fibres aligned with their long axes parallel to the rod axis. X-ray diffraction indicated that the Cr fibres had a strong ⟨110⟩ fibre texture. The mechanical properties of the composite were measured by tensile testing over the temperature range −70 to 600°C. Examination of fibre fracture and fibre-matrix debonding at and near the tensile test fracture surfaces indicated that a transition from localised to global damage occurred between 300 and 400°C.

1. Introduction

Over the past 25 years, a class of Cu conductive materials (Cu-X) possessing excellent mechanical and electrical properties, have been developed within the framework of metal matrix composites [1–10]. These composites, comprise copper (fcc) with an element X (where X is a bcc metal immiscible in Cu such as Nb, Cr, Fe, Mo or V). The composites are formed by mechanical working (swaging, extrusion, rolling or drawing) of ductile two phase mixtures prepared by liquid phase sintering, casting or powder metallurgy. The fact that Cu-Cr can be co-deformed, in spite of the brittle nature of pure Cr at room temperature, was first studied by Funkenbusch *et al*. [11, 12] in a Cu-17 vol% Cr alloy drawn into wires. In service, the strategy is that the fibrous metal X can bear the higher fraction of load while the surrounding Cu matrix gives good conductivity and ductility. Considerable strengthening also accrues from the microstructural refinement of both phases. The Cu-Cr system is of particular interest because of the limited solubility of Cr in Cu, relatively low cost and good microstructural stability at high temperature. This makes Cr an excellent reinforcing metal for Cu based *in situ* composites.

In these composites, the volume fractions of the secondary phase are relatively low (≤ 0.2) so that it exists as isolated particles in a powder compact or isolated dendrites in a casting. This kind of material is often termed an "*in situ* composite" because during deformation processing both phases deform with the result that filament with very large aspect ratios are formed in a matrix material. The key factor in the formation of these composites depends on the starting material. The first step in the preparation of these composites is the manufacturing of a billet of a two-phase alloy. The initial shape (spherical, dendritic, globular, etc.) of the phases in the billet is not very important because when a very large deformation strains are employed, an aligned fibres of the secondary phase would be produced.

The room temperature mechanical properties of copper based composites have been extensively studied in recent years, and some investigators have examined the effect of elevated temperature annealing on their room temperature mechanical properties. However, few studies have reported on the tensile behaviour of such composites at elevated temperature. The load partitioning ratio between the matrix and reinforcement normally remains constant as long as both components behave in

*Current address: Department of Semis and Rods (Technical), Corus Construction & Industrial, PO Box 1, Brigg Road, Scunthorpe, North Lincolnshire, DN16 1BP, UK.

†Author to whom all correspondence should be addressed.

a linear elastic manner. Upon plastic deformation, this ratio changes ideally so that the reinforcing phase carries a higher portion of the applied load. However, with increasing stress in the reinforcement, it may fracture or debond from the matrix, thus reducing the load it carries and reducing the overall load bearing capacity of the composite which eventually will lead to composite failure.

The aim of the current study was therefore to characterise the thermomechanical response of a Cu-Cr composite over a wide range of temperatures, both in terms of composite properties, and the nature and extent of any damage mechanisms occurring within the composite.

2. Experimental procedure

2.1. Materials

The Cu-10 vol% Cr *in situ* composite used in this study was produced by vacuum casting at 1870 K by Essex Metallurgical Limited. The final ingot was approximately 14.5 mm in diameter. It was then hot forged at 1170 K and swaged at room temperature into 3 mm diameter rod. Deformation reduction can be expressed in terms of true strain η by:

$$\eta = \ln\left(\frac{A_0}{A_f}\right)$$

where A_i is the initial cross sectional area of the specimen, and A_f is the final cross sectional area after deformation. This true strain must be greater than around 3 (equivalent to a reduction in area of approximately 95%) to achieve any strengthening effect in the composite. In the 3 mm rod, the deformation strain η was 3.15 which was approximately 95.6% reduction in area.

2.2. Material characterisation

Tensile tests were carried out on a Hounsfield machine at temperatures ranging from -70 to 600°C under displacement control at a rate of 16.7 μm/s, with the Cr fibres parallel to the loading direction. Tensile test pieces used were 70 mm long and 3 mm in diameter. To ensure that the tensile test samples fractured in the central region, the middle section of 20 mm length was machined into a square cross section with a width of 2.2 mm. The axial strain was monitored by using a video extensometer (ME-46 Full Image Videoextensometer). For tests performed at elevated temperatures, a 3 kW heating element was used, with the specimens and attached equipment given 30 min at elevated temperature before testing began. To ensure a uniform heat distribution on the specimen, 4 ceramic heaters were arranged to form a circle around it. No load was applied to the specimen during heating, and the specimen was removed immediately after testing to minimise any creep effects. Cryogenic tests were performed by spraying liquid nitrogen directly onto the specimen. The supply of liquid nitrogen to the specimen was automatically cut-off when the desired temperature (-70°C) was achieved as measured by a thermocouple in contact with the sample. The accuracy of this method was about ± 5°C.

X-ray diffraction (XRD) was performed on a Siemens D5000 diffractometer using a Huber closed Eularian cradle. Cu K_α radiation was ($\lambda = 0.1541$ nm) on transverse sections of the material at $\eta = 3.15$. Since the Cr phase is the minority phase in this composite, 12 transverse specimens were arranged closely to each other to generate a more accurate data.

The fracture surfaces of the test specimens were subsequently examined by SEM to determine the various failure mechanisms that operate during tensile testing of the composites. Selected fractured specimens were also sectioned along their tensile axes and prepared for metallographic examination. In order to characterise the extent of damage as a function of temperature, micrographs were taken of the polished samples near the fracture surface (~2 mm from the fracture surface), and far from the fracture surface (~8 mm from the fracture surface) and at an intermediate distance (~4 mm from the fracture surface).

3. Results and discussion

3.1. Microstructural evolution

In the as-cast state, the Cr is in a dendritic form as shown in Fig. 1. The dimension of dendritic Cr (including dendritic arms) varies from 20–100 μm. Because the difference in density is relatively slight ($\rho_{Cu} = 8.93$ g cm^{-3} and $\rho_{Cr} = 7.14$ g cm^{-3}) gravitational segregation of the primary dendrites during casting is not a major concern. During subsequent deformation, the Cr dendrites elongated into fibres parallel to the swaging axis (Fig. 2). The good interfacial bonding between the Cu and Cr makes the large deformation possible without any interfacial failure, which is one of the advantages of *in situ* composites. It can be seen that after deformation, the original morphologies of dendritic Cr and equiaxed Cr could not be distinguished. A small amount of what appears to be some residual equi-axed Cr can be seen. The mean thickness of the Cr fibres is 2 μm with an aspect ratio of 25:1 (dimension parallel to the rod axis: dimension perpendicular to the rod axis) as measured from many SEM micrographs.

XRD texture analysis of the material at $\eta = 3.15$ indicated that the Cr had the expected ⟨110⟩ fibre texture and Cu a mixed ⟨111⟩/⟨200⟩ as shown in Fig. 3. The Cu texture is the stronger. The ⟨110⟩ fibre texture in the Cr limits the deformation of the Cr fibres to just two of the four ⟨111⟩ slip directions, as shown in Fig. 4. This plane strain mode produces Cr fibres that have elliptical, rather than circular, cross sections as seen in a transverse section (Fig. 2). This tendency becomes quite pronounced at high η values in Cu-X composites, but it is relatively modest in these composites, since their maximum deformation was only $\eta = 3.15$. Nevertheless, this plane straining effect results in a larger Cu-Cr interfacial area than would be present if the Cr phase were more nearly cylindrical. This larger Cu-Cr interfacial area will lower the effective shear stress at the Cu-Cr interface by distributing the shear force over a larger area, and thus this filament morphology may be less likely to experience matrix-filament separation than would be the case in a classic composite containing cylindrical filaments.

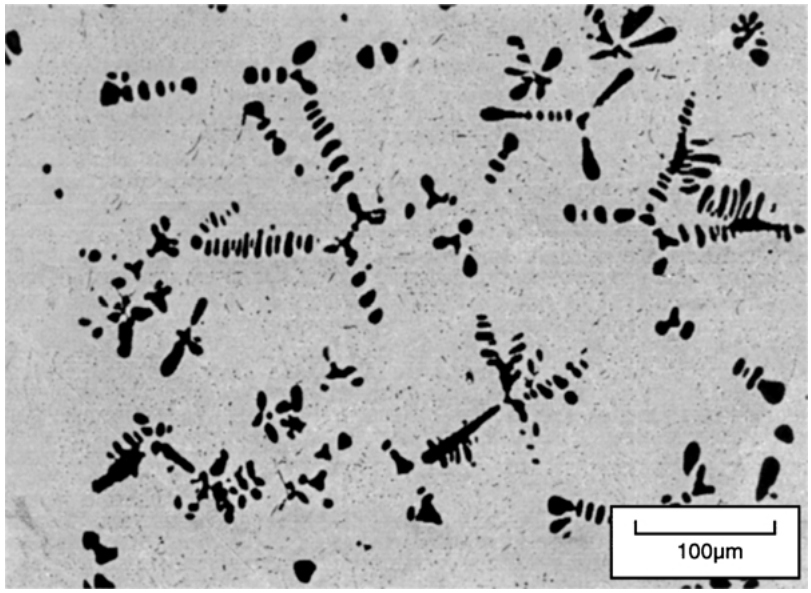

Figure 1 SEM image of the as-cast composite, the Cu matrix having being selectively etched away.

Figure 2 Three-dimensional representation of the microstructure from backscattered SEM micrographs after deformation to $\eta = 3.15$. The Cr fibres (darker phase) lie parallel to the specimen rod (swaging) axis.

3.2. Mechanical properties

The stress-strain plots obtained at nine testing temperatures are shown in Fig. 5. These plots show that the presence of the Cr fibres increases the room temperature (RT) yield strength of the material by 77% and the ultimate tensile strength of the material by 43% compared to those of pure Cu. These are typical of the strengthening effects seen in other Cu based composite at this η level. The ductility of the material is relatively low at all temperatures and decreases as the temperature decreases.

As expected the addition of Cr results in a significant increase in the Young's Modulus and load bearing capacity of the composite with a corresponding loss in ductility. The Young's Modulus of the composite may be calculated using the isostrain loading or isostress loading conditions. The Young's modulus predicted assuming the "Rule of Mixtures" (ROM) isostrain loading condition ($E_{\text{composite}} = E_{\text{f}}V_{\text{f}} + E_{\text{m}}(1 - V_{\text{f}})$) is greater than that of isostress loading condition ($E_{\text{composite}} = E_{\text{f}}E_{\text{m}}/(V_{\text{f}}E_{\text{m}} + (1 - V_{\text{f}})E_{\text{f}}$). Here, E_{f} and E_{m} are the Young's modulus of fibre and matrix respectively, and V_{f} is the fibre volume fraction. Substituting $E_{\text{f}} = 280$ GPa, $E_{\text{m}} = 135$ GPa, and $V_{\text{f}} = 0.1$ into this expression gives a composite modulus of 149.5 GPa for the isostrain loading condition and 142 GPa for the

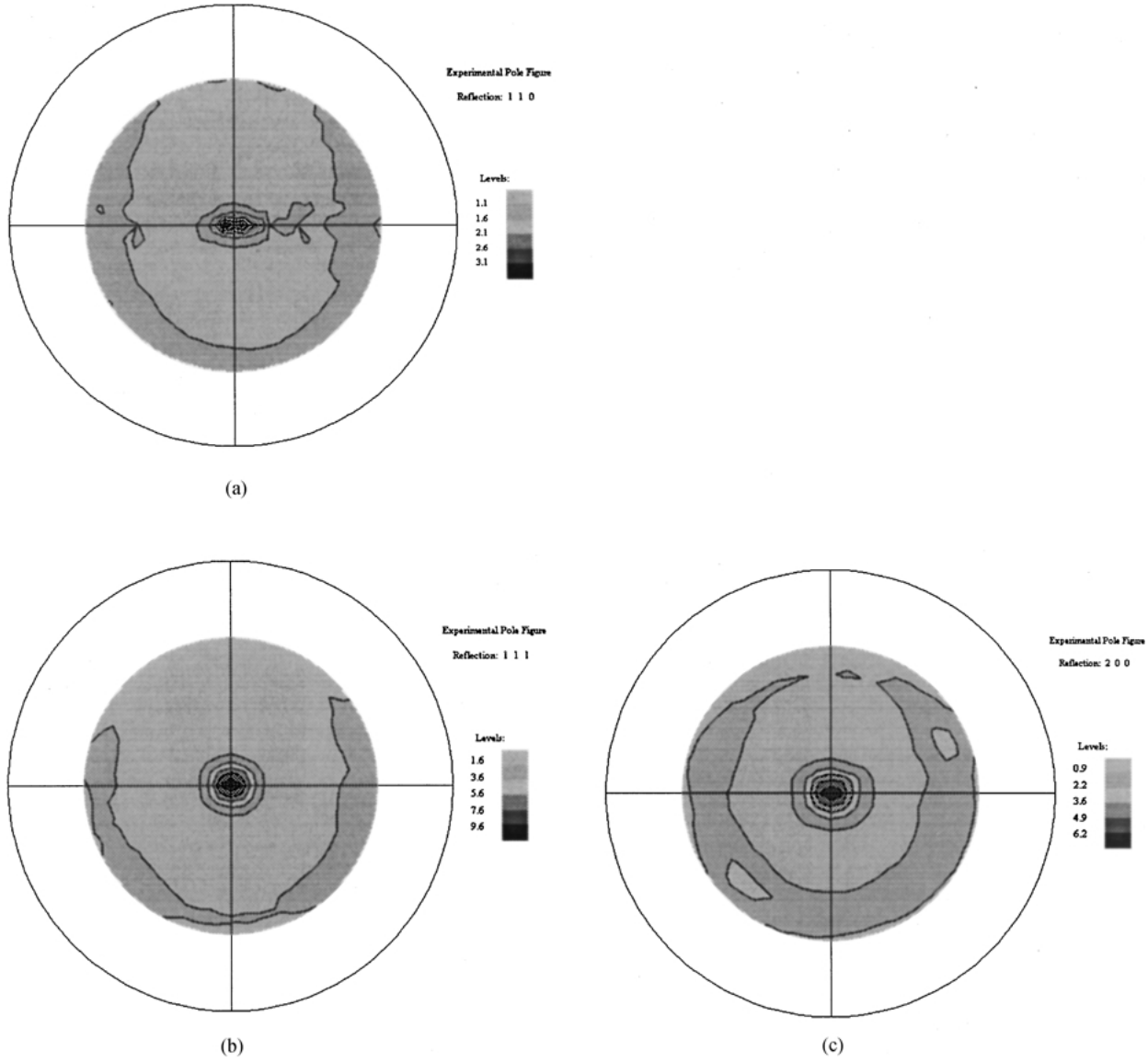

Figure 3 XRD texture analysis pole figures for (a) ⟨110⟩ Cr, (b) ⟨111⟩ Cu, and (c) ⟨200⟩ Cu.

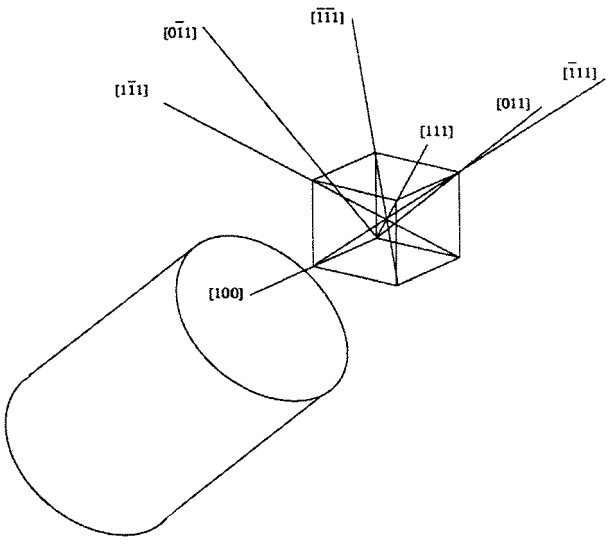

Figure 4 In a bcc crystal with a [110] direction aligned parallel to the swaging direction, two of the four ⟨111⟩ slip directions are perpendicular to {110} and so have no driving force for slip (Schmid factor = 0). Thus, all slip is limited to the remaining two directions, the [111] and the [$\bar{1}$11] resulting in a plane straining filament with the unequal dimensions.

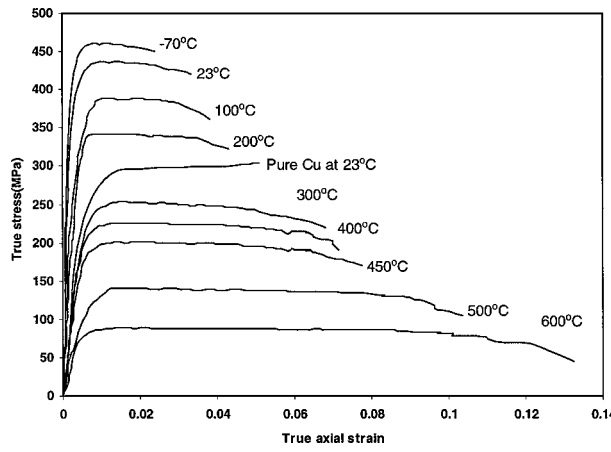

Figure 5 Stress/strain response for similarly processed unreinforced copper (RT) and Cu-10 vol% Cr composite tested from −70 to 600°C.

isostress loading condition. Since the aspect ratio of Cr fibres is fairly high and fibres are aligned parallel to the loading axis, one would expect the actual modulus to be close to the isostrain prediction. The slope

of the elastic region in Fig. 5 for the composite tested at room temperature is 142 GPa, which is close to the calculated isostress value. However, this does not necessarily mean that Cr fibres and Cu matrix are loaded in series since the predicted values are within the range of experimental error. The experimental modulus from mechanical testing is likely to be a little lower than the real modulus because machine modulus is usually reflected in the experimentally observed modulus and the possibility for early macro-yielding.

Models for predicting tensile strength are generally oversimplistic. The ROM implicitly assumes there is no mechanical interaction between components other than the transfer of load across the interface between them. Blind application of the method predicts a room temperature tensile strength of 321 MPa ($\sigma_m = 280$ and $\sigma_f = 690$ MPa). However simple composite models do not really include the extent of microstructural refinement since the unreinforced materials are unlikely to have the same level of microstructural refinement as for the composite. The ROM value is lower than the 430 MPa measured tensile strength of the composite at room temperature. The difficulty in obtaining pure Cr tensile strength data at temperatures below 300°C make ROM estimates somewhat unreliable, but even if one allows for considerable variation in the σ_f value, the ROM predictions are still low. Cu-X composites frequently have strengths higher than ROM predictions for reason that have been discussed at length elsewhere. Positive deviations from the rule of mixtures occur, with the magnitude increasing with increasing strain [12]. Observed tensile strengths eventually approach the theoretical limit at drawing strain of $\eta = 9$–10 and the fibre diameters of tens of nanometers. Dislocation density was found to increase rapidly with strain until the fibre size reaches very small values (tens of nanometers) at which point it decreases sharply and some fibres appeared nearly dislocation free. This behaviour was due to the reduction of interphase spacing with strain and must involve comparatively long range (e.g., dislocation/dislocation) rather than short range (i.e., atomic scale) interactions.

The existing models for microstructural strengthening of Cu-X composites are difficult to apply to the Cu-10 vol% Cr composite data of the present study, since tensile strength was measured only at one value of η (=3.15) at which the interfilamentary spacing is greater that the microstructural scale of Cu matrix [13]. Therefore, both barrier strengthening models (Spitzig and coworker) and dislocation storage models (Courtney and coworkers) cannot be used to predict the strength of Cu-Cr of the present study since the microstructural scale (50–300 nm) of highly deformed composite is much smaller than that (2–5 μm) of the present study.

3.3. Microstructural damage accumulation

Almost no damage was observed in the composites after swaging. As a result, the effect of process induced on the subsequent damage evolution during tensile testing of this composite has been neglected by this study.

3.3.1. Low temperature straining

Microstructural observation of longitudinal sections of the fractured specimens show that the damage in the composite was highly localised near the fractured surface as shown in Fig. 6. Damage was seen in the form of reinforcement cracking. Fibre cracking is severe and frequent at −70°C, suggesting the ductility of Cr fibres decreases rapidly below room temperature.

3.3.2. Room temperature straining

The evidence of longitudinal sections and fractography is consistent with previous internal stress measurements [14] that suggest both phases co-deform during tensile testing. This in itself is not surprising since the samples were previously co-deformed by cold swaging so that one might expect both phases to reach their tensile yield criterion at approximately the same composite tensile strain. Fig. 7 shows ductile dimpling of the Cu matrix along with some evidence of necking of the Cr fibres, most of which lie at the base of the matrix dimples. The mechanism of failure is clear from the associated longitudinal section taken near the fracture surface (Fig. 8). Matrix voids have formed in regions of fibre ends or where fibres have necked to failure. No evidence of Cu-Cr separation or early brittle Cr fracture is visible in this fractograph or in several others taken of this region. Such failure sites were rare even in the immediate vicinity of the fracture surface and were not found at all farther from it.

3.3.3. Elevated temperatures

The micrographs shown in Figs 9–11 were taken from specimens tested at 300°C, 400°C, and 500°C respectively. In all cases damage in the form of matrix cavitation is primarily located near the ends of Cr fibres. There was also some evidence of matrix cavitation at the interface between the Cu matrix and the Cr reinforcement. In all cases, failure occurred by the coalescence of cavities. The level of damage was found to increase as the temperature increases. At temperatures up to 300°C, microstructural observation of longitudinal sections immediately beneath the fracture surface showed that the damage in the composite was fairly localised. Further from the fracture surface, not much damage was seen (Fig. 9). For the composite tested at 400°C, the level of damage was slightly greater near the fracture surface than at 300°C but was also found to be more homogeneous extending throughout the gauge length as shown in Fig. 10. One interesting observation is that cracks in Cr fibres surrounded by intact Cu matrix were rarely observed at high temperature unlike at low temperatures (Fig. 6), suggesting that Cr fibres are sufficiently ductile under these conditions. Damage was extensive and the primary damage mechanism was void nucleation at the fibre ends although some fibres were found to neck creating matrix voids. These features were accentuated in the sample tested at 500°C so that damage was extensive and spread throughout the gauge length.

In order to understand the failure mechanism of Cu-Cr composites, it is necessary to figure out whether

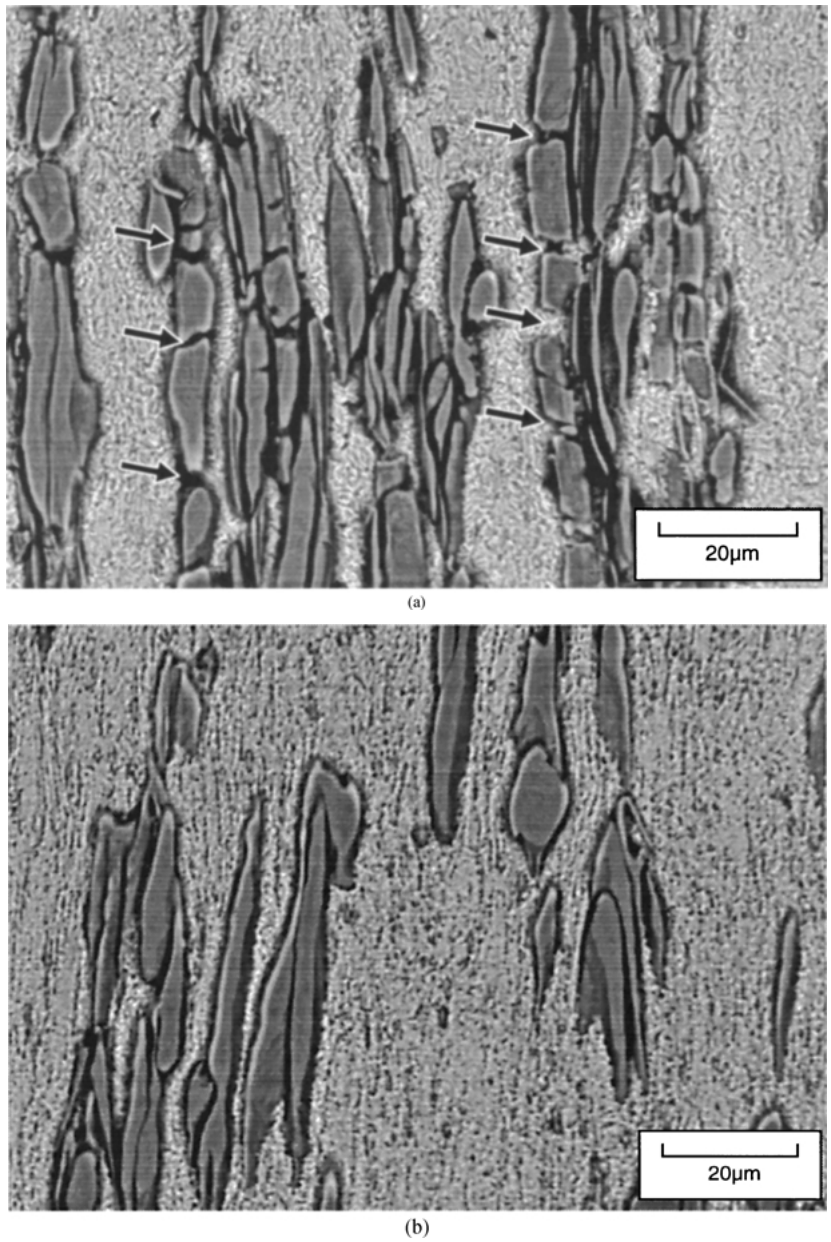

Figure 6 Typical micrographs obtained (a) near the fracture surface and (b) remote from the fracture surface of Cu-10 vol% Cr specimen tested at −70°C: note that damage is localised near the fracture surface in the form of reinforcement cracking (indicated by the arrows).

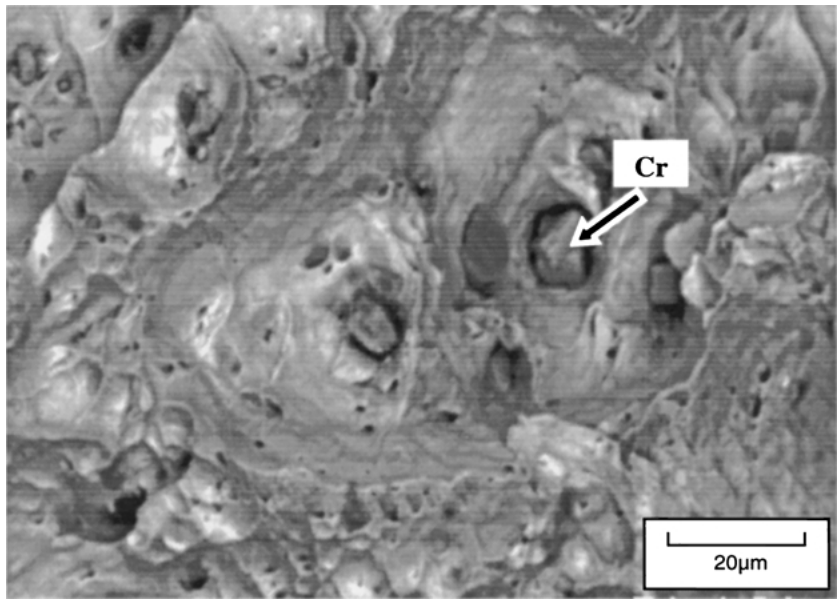

Figure 7 Typical micrograph for the Cu-10 vol% Cr specimen tested at room temperature.

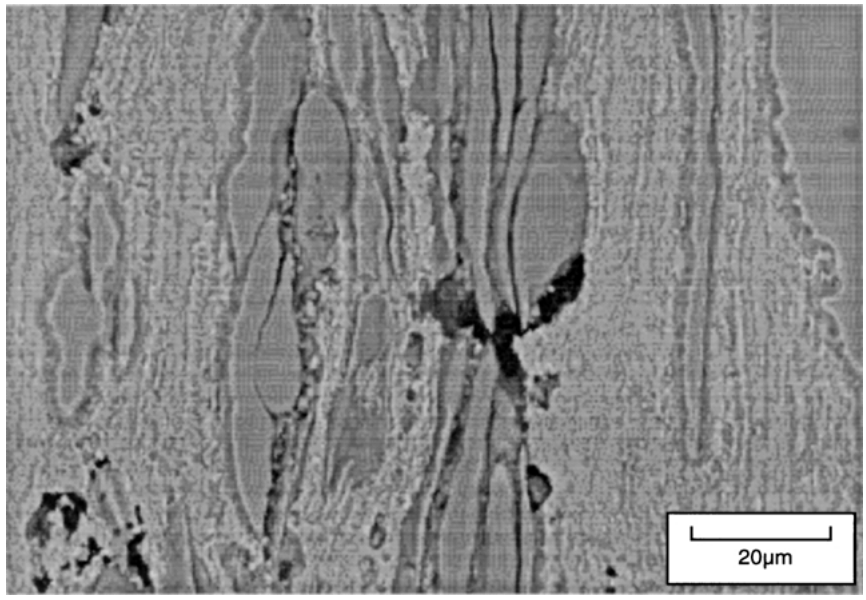

Figure 8 Longitudinal section of the fractured Cu-10 vol% Cr specimen (2 mm away from the fracture surface).

the voids in the Cu matrix precede the failure of the Cr fibres or vice versa. The failure sequence can be deduced by observing the damage accumulation with increasing strain. Since the strain is more extensive near the fracture surface, it may be assumed that the appearance of the damage far away from the fracture surface resembles the early stages of the failure. Voids were also occasionally observed between the ends of two aligned Cr fibres at which the local stress is high [15, 16]. A careful examination of the micrographs far from the fracture surfaces (Figs 10c–11c) suggests that voids develop first near the ends of fibres before the necking failure of fibres at high temperatures. Fibre necking often occurs in regions for which strain is accentuated by nearby fibres end-related matrix voiding. The appearance of major cracks in Fig. 11a also suggests that the final crack was formed by a conventional void coalescence and link-up process. At high strains and temperatures localised voiding contributes significantly to the total strain achieved.

4. Discussion

The performance of a composite is strongly dependent upon the efficiency with which load is transferred to the reinforcement during deformation. This is determined by the misfit generated between the two phases. In a MMC, elastic and/or plastic heterogeneities generate the misfits, which in turn results in load transfer to/from the reinforcement. The resulting high reinforcement stresses, and high local stresses within the matrix near the reinforcement, may then promote stress relaxation mechanisms. The operation of such stress relaxation mechanisms, which may involve microstructural modification such as dislocation rearrangement near interface regions and phase boundary sliding and microstructural damage such as reinforcement fracture and matrix cavitation, will then act to reduce the misfit and transfer load back to the matrix. Therefore, microstructural observations on the extent of damage in a fractured specimen can provide an indication whether load transfer has occurred.

At room temperature, both phases (Cu and Cr) are able to deform plastically [14]. A previous study has shown that the onset of plasticity results in a strain misfit between the phases which acts to transfer load *towards* the Cu phase [14]. In other words the Cr deforms slightly more and slightly earlier than the Cu. This surprising result was borne out by final residual strains. The co-deformation processing prior to testing had meant that the Cr phase reached the yield locus at approximately the same strain as the Cu phase due to a combination of its high stiffness and the probable presence of swaging induced residual stresses. A higher stiffness for the Cr phase relative to the Cu phase meant that although the two phases deformed approximately equally, the Cr phase had the larger plastic component resulting in load transfer from Cr to Cu with increased straining. In the current work, the longitudinal sections taken at room temperature are suggestive of fairly uniform strain, except in the immediate vicinity of the fracture surface. In this region a damage site (caused by a necked filament or a filamentary end) soon becomes critical and grows to catastrophic failure.

At high temperatures, on the other hand, plasticity would appear to be uneven, resulting in high stresses in the fibres which cannot ultimately be borne by the matrix near the filament ends. This results in the nucleation of many small voids. These remain relatively stable, growing both in size and number until finally void coalescence occurs giving rise to failure. The more homogeneous distribution of voids with increasing temperature is thought to be associated with increase of strain rate sensitivity and a decrease in strength in the Cu matrix with increasing temperature. The strain rate sensitivity of pure metals tends to rise linearly with the absolute temperature [17, 18]. It is well known that the deformation and damage become more homogeneous with increasing strain rate sensitivity [19, 20].

At low temperatures, the phases would strained equally but, the constraint is not sufficient for ductile flow in the Cr phase. Consequently, most of the damage occurs in the form of reinforcement cracking. This

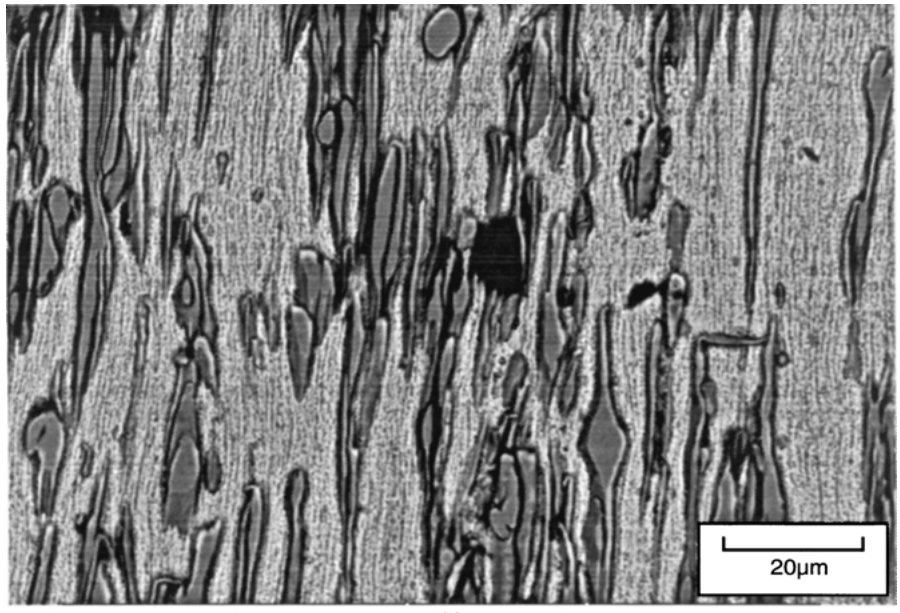

(a)

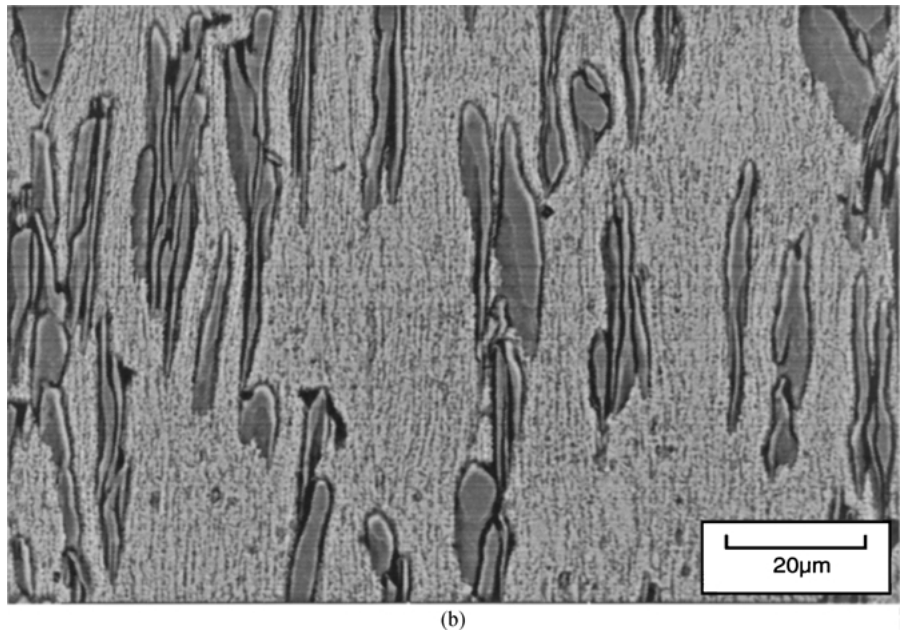

(b)

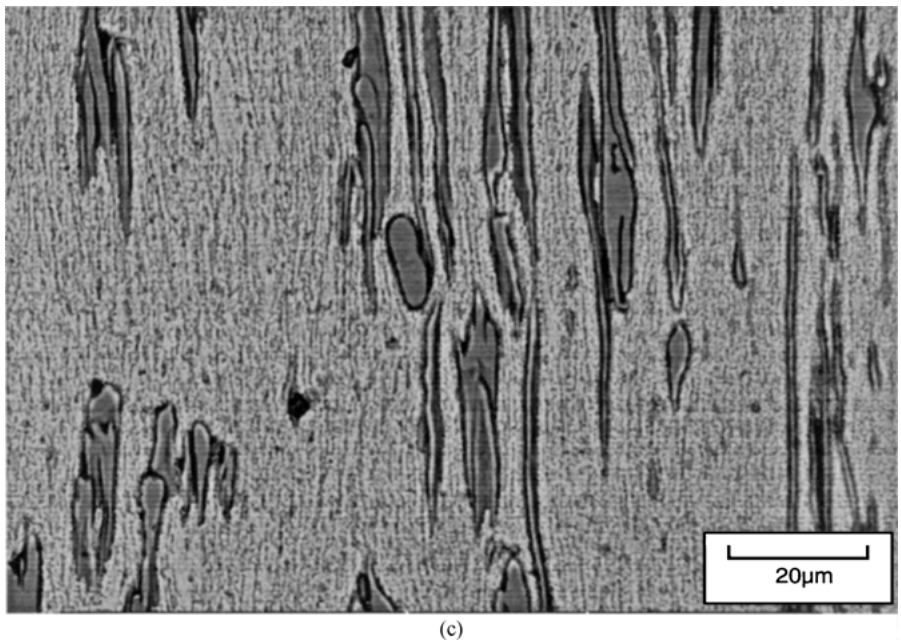

(c)

Figure 9 Typical micrographs taken from (a) near the fracture surface and (b) intermediate distance from the fracture surface (c) far from the fracture surface for Cu-10 vol% Cr specimen tested at 300°C.

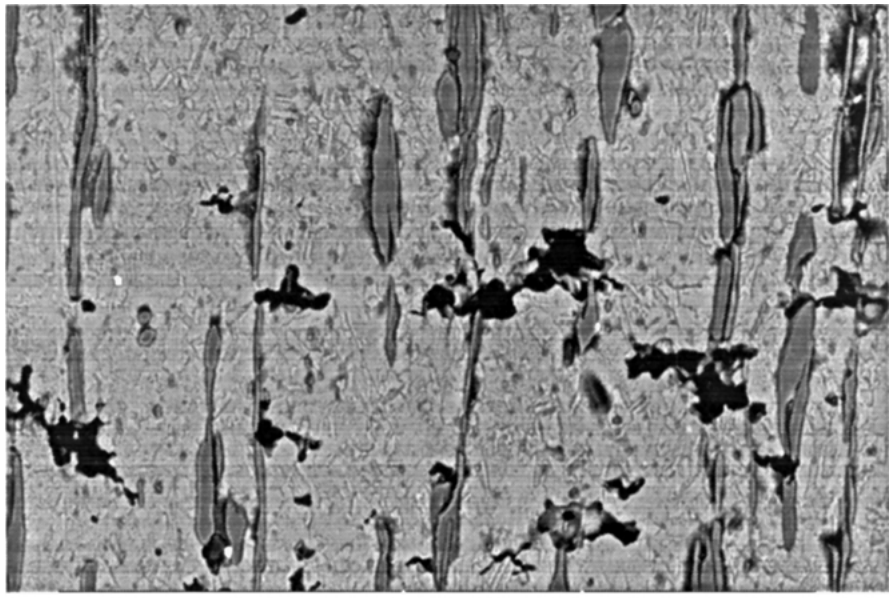

(a)

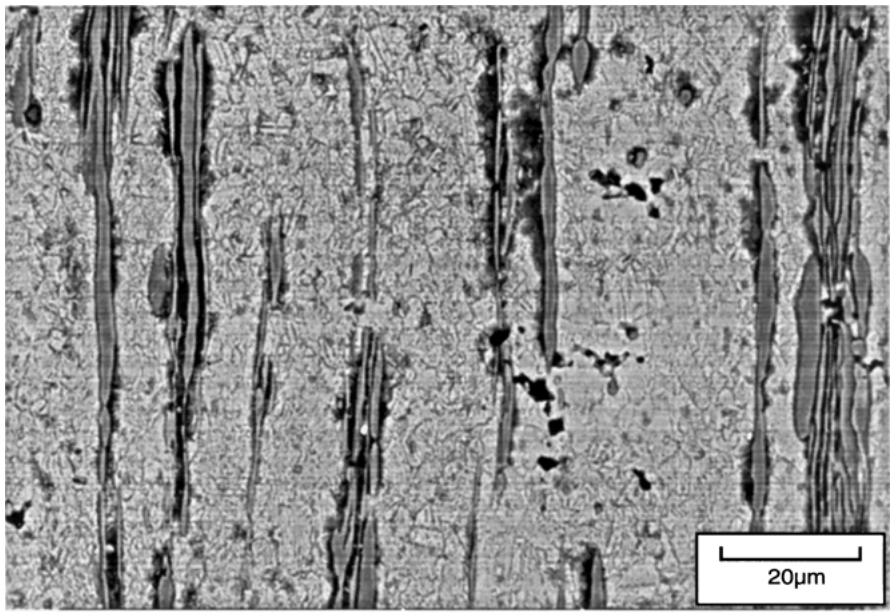

(b)

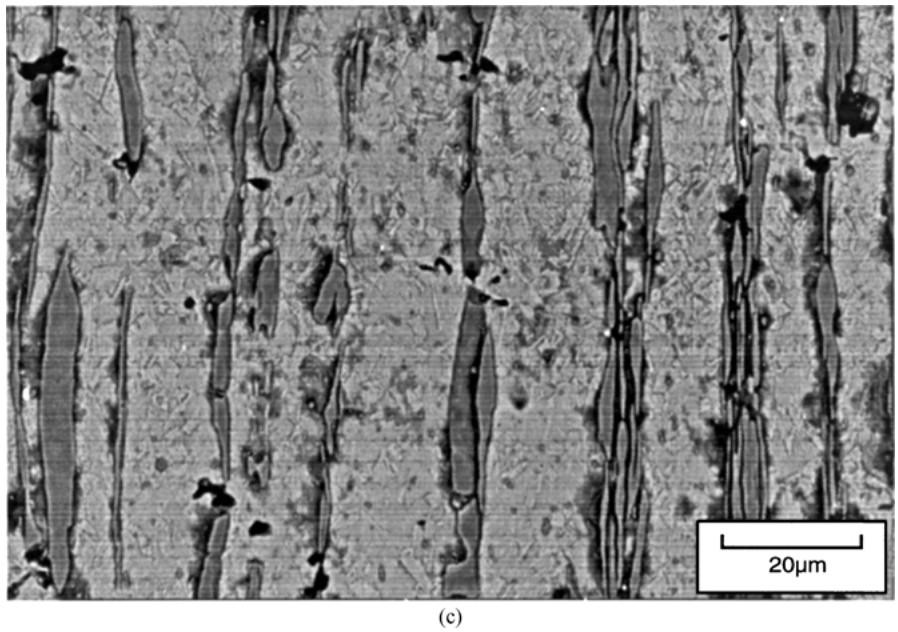

(c)

Figure 10 Typical micrographs taken from (a) near the fracture surface and (b) intermediate distance from the fracture surface (c) far from the fracture surface for Cu-10 vol% Cr specimen tested at 400°C.

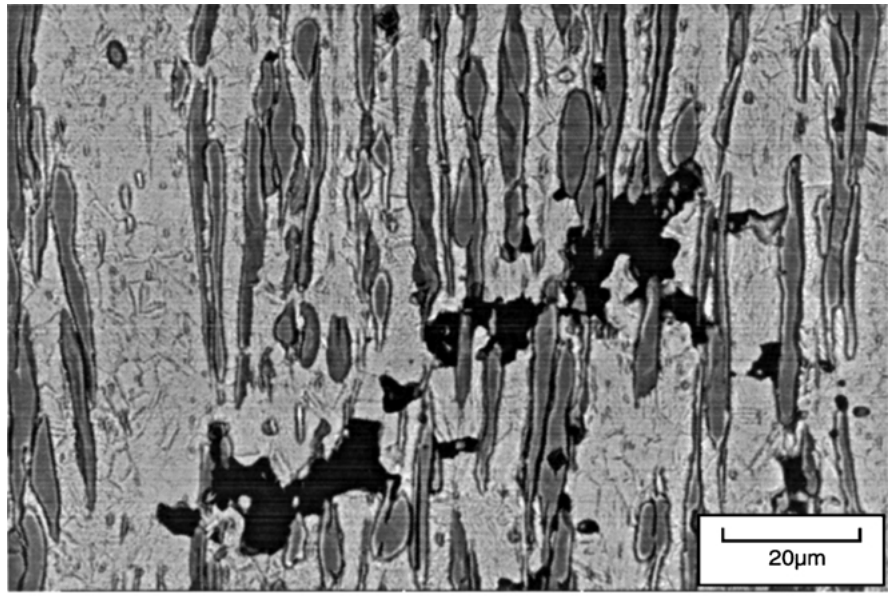

(a)

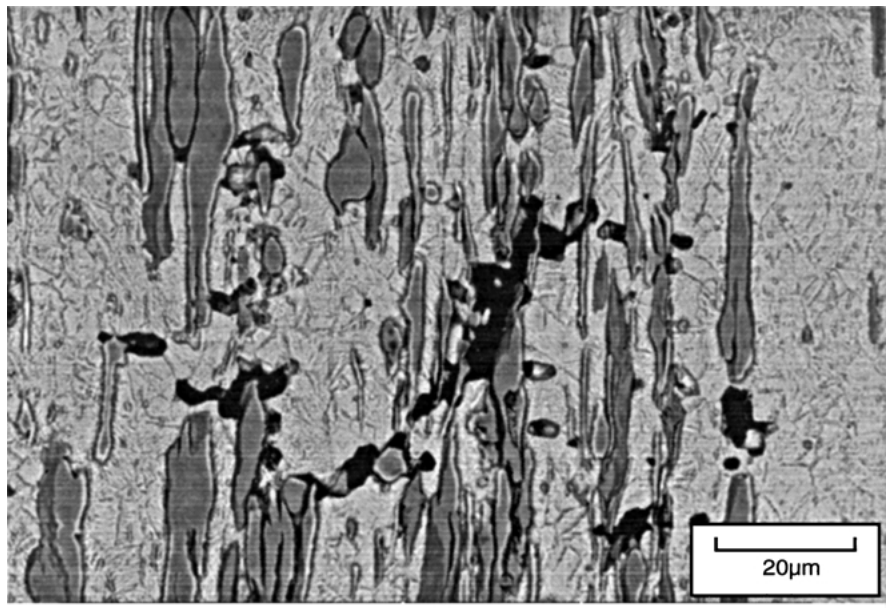

(b)

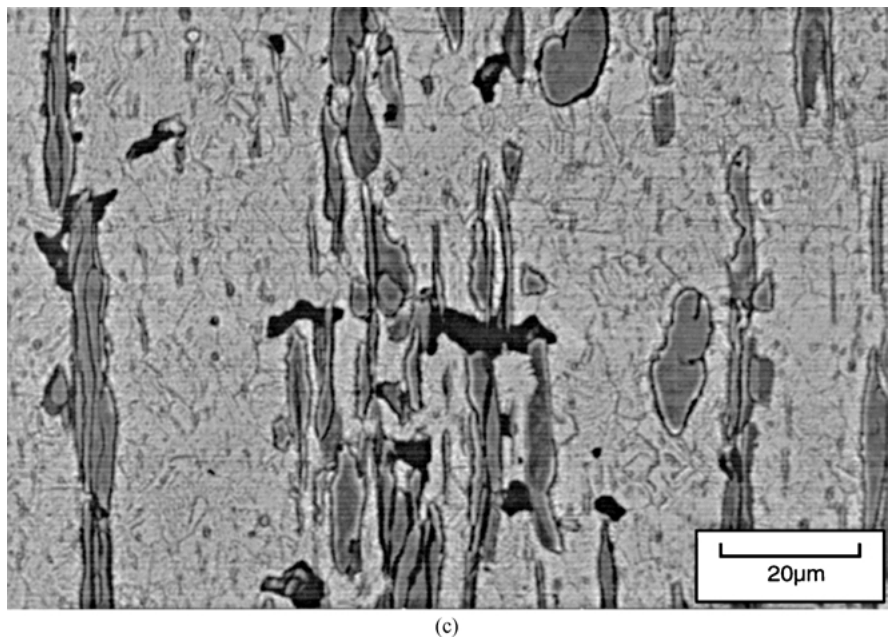

(c)

Figure 11 Typical micrographs taken from (a) near the fracture surface and (b) intermediate distance from the fracture surface (c) far from the fracture surface for Cu-10 vol% Cr specimen tested at 500°C.

occurs before the critical hydrostatic stress required for cavitation in the matrix due to the brittleness of the Cr phase at this temperature. This damage mechanism in the composite has been modelled by Evensen and Verk [21]. The load is transferred back to the Cu matrix after the reinforcement fractures. This means that at the region of the fractured reinforcement, Cu will deform at a higher local strain rate than the global strain rate. The voids (formed between the Cr fracture points) will grow laterally because there is a plastic zone [21] which extends sideways into the Cu matrix which is no longer constrained by the reinforcement. Failure then occurs when adjacent voids combine. Microstructural observations showed that the damage was concentrated near the fracture surface, which suggests that this form of damage is catastrophic, and cannot be accommodated in the composite without rapidly leading to the onset of failure. The ductility of this composite at this temperature is therefore expected to be low, which is consistent with the low measured failure strain.

5. Conclusions

At room temperature, co-deformed Cu-10 vol% Cr composite has superior yield strength over similarly processed unreinforced Cu. With increasing strain, a monotonic rise in yield stress and a concomitant decrease in ductility is observed for Cu-10 vol% Cr composite.

During room temperature tensile testing, both phases yield plastically. As the test temperature is increased, the Cu becomes much more plastic (softer) than the Cr. As a result of this, a significant misfit is generated between the matrix and reinforcement during deformation, and the Cr is preferentially loaded. This is consistent with the microstructural observations which show that damage occurs preferentially near fibre ends as the test temperature is increased. With increasing temperature, a transition was observed from co-deformation and localised damage at the fracture surface to inhomogeneous deformation but homogeneously distributed damage. This has been observed for other ductile matrix composite systems as a function of temperature.

The concept of localized and global damage are useful to explain the temperature dependency of the damage distribution and thus ductility. When fracture of a fibre leads to significant stress concentration on the neighbouring fibre, then the adjacent fibre could fail and set up a chain of failures leading to the ultimate failure of the composite. This type of damage is termed localised damage. The composite strength is then dominated by a few potential damage sites and the full fibre bundle strength is never realized. If global damage controls the behaviour of the material, then the occurrence of a damage event relaxes the stresses in that area of microstructure. As a result this stress will be distributed throughout the composite. Therefore the subsequent damage event is more likely to occur in another region of the specimen, as the stress in the area of the initial damage is relaxed. This results in a homogeneous distribution of damage within the composite. Clearly, global damage conditions are desirable for high fracture toughness because it leads to greater ductility and damage tolerance.

In the present study, a clear transition in the distribution of damage occurs from 300°C to 400°C. At higher temperatures deformation is greater in the Cu phase and peak stresses are relaxed by increased plasticity and diffusion rates, so that local stresses within the Cu matrix are more easily relaxed after a void is formed. It can be concluded that as the temperature is increased, there is a distinct change from localised to global damage within the composite. The more homogeneous distribution of Cu-Cr composites with increasing temperature is thought to be associated with a decrease in Cu strength and an increase of strain rate sensitivity.

Acknowledgements

One of the authors (K.L. Lee) is grateful to Mr. G. R. O'Connor of Leicester University for his support and encouragement during the duration of this research. Thanks are also due to Mr. K. A. Roberts of Cambridge University for preparing the composite materials.

References

1. H. P. CHESKIS and R. W. HECKEL, *Met. Trans.* **1** (1970) 1931.
2. A. M. RUSSELL, L. S. CHUMBLEY and Y. TIAN, *Advanced Eng. Mater.* **2** (2000) 11.
3. K. L. LEE, H. E. CARROLL and A. F. WHITEHOUSE, *Mater. Sci. Tech.* **16** (2000) 811.
4. K. L. LEE, S. I. HONG and A. M. RUSSELL, submitted to *Metal Mater Trans. A.*
5. K. L. LEE, A. F. WHITEHOUSE and A. C. F. COCKS, *ICCM* **12** (1999).
6. K. L. LEE, submitted to *Scripta Mater.*
7. K. L. LEE, S. I. HONG and A. M. RUSSELL, submitted to *Scripta Mater.*
8. K. L. LEE, submitted to *Acta Mater.*
9. S. I. HONG, M. A. HILL, Y. SAKAI, J. T. WOOD and J. D. EMBURY, *Acta Metall. Mater.* **43**(9) (1995) 3313.
10. C. BISELLI and D. G. MORRIS, *Acta Mater.* **44**(2) (1996) 493.
11. P. D. FUNKENBUSCH, T. H. COURTNEY and D. G. KUBISCH, *Scripta Metall.* **18**(10) (1984) 1099.
12. P. D. FUNKENBUSCH and T. H. COURTNEY, *Acta Metal.* **33**(5) (1985) 913.
13. S. I. HONG, *Scripta Mater.* **39**(12) (1998) 1685.
14. K. L. LEE, A. F. WHITEHOUSE, P. J. WITHERS and M. R. DAYMOND, *Mater. Sci. Eng.* A **348** (2003) 208.
15. S. R. NUTT and A. NEEDLEMAN, *Scripta Metal.* **21**(5) (1987) 705.
16. S. R. NUTT and J. M. DUVA, *ibid.* **20**(7) (1986) 1055.
17. J. D. LUBAHN, *Trans. Aime* **185** (1949) 702.
18. K. W. LEE, S. K. KIM, K. T. KIM and S. I. HONG, *J. Nuc. Mater.* **295**(1) (2001) 21.
19. S. I. HONG, *Scripta Mater.* **40** (1999) 217.
20. *Idem.*, *Mater. Sci. Eng.* A **79**(1) 1986 1.
21. J. D. EVENSEN and A. S. VERK, *Scripta Metall.* **15** (1981) 1131.

Received 22 October 2002
and accepted 3 April 2003